

A new type photonic crystal fiber with high birefringence*

LOU Shu-qin*, JIAN Wei, REN Guo-bin, and JIAN Shui-sheng

Institute of Lightwave Technology, Beijing Jiaotong University, Beijing, 100044, China

(Received 20 May 2005)

In this paper, a new type of photonic crystal fiber with high birefringence is proposed and analyzed with a full-vector model based on the super-lattice and the plane-wave expansion model. Due to the two different sizes of the holes introduced into the cladding of the PCF, the fiber is two-fold rotational symmetry and appears to be with high birefringence. Numerical results demonstrate that a modal birefringence at wavelength $1.31 \mu\text{m}$ is 1.8×10^{-3} in the PCF with $\Lambda = 2.55 \mu\text{m}$, $d_1/\Lambda = 0.3$ and $d_2/\Lambda = 0.833$. A near 200 nm SPSM region within the wavelength range from $1.4 \mu\text{m}$ to $1.6 \mu\text{m}$ is obtained.

CLC number: TN253 Document code: A Article ID: 1673-1905(2005)01-0024-03

High performance polarization-maintaining fibers (PMFs) have potential for a number of applications such as high bit rate communication system, PM fibre loops for gyroscopes and so on. The index-guiding PCFs are characterized by a series of holes running throughout the length of the fiber arranged in a microscale structure around a high index core. This offers a new possibility to create high birefringence in the index-guiding PCFs, because the stack-and-draw process allows the formation of the required symmetric or asymmetric microstructure and the index contrast of the index-guiding PCFs is higher than that of conventional fibers. Through changing the shape and size of air hole^[1-2], high birefringence PCF can be realized and its modal birefringence could reach 10^{-3} order of magnitude.

Based on the near elliptical core PCF^[3], eight big air holes are introduced near the core region along direction x , and a new type of high birefringence PCF having a W-shaped effective index profile along the axis y , as shown in figure 1, is formed. The properties of this PCF are analyzed by the combination of super-lattice full vector model and plane wave method.

As shown in figure 1, the sizes of big holes and small holes are characterized by the hole diameter d_2 and d_1 , respectively, and the hole pitch is represented by Λ . The parameter d_2/d_1 is arranged larger than 1, which results in a W-shaped effective index profile along the axis y . Polarization maintaining fiber with a W-shaped refractive index profile has different cutoff wavelengths for the two polarized fundamental mode, as the degeneracy of the fundamental mode is lifted^[4].

To model the polarization properties, the scalar approximation becomes inadequate. Thus a full vector model has to be employed to accurately predict sensitive

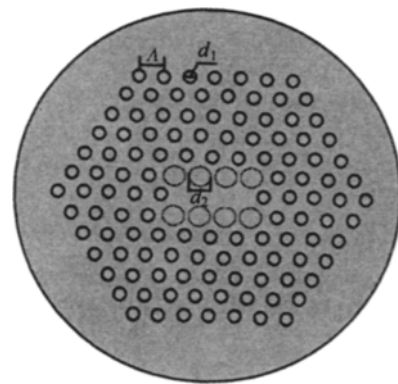


Fig. 1 Transversal cross section of high birefringence PCF proposed

properties.

Assuming that the PCF be lossless and uniform in the propagation (z) direction, we focus on the transverse mode field distribution $e_x(x, y)$ and $e_y(x, y)$, which satisfy a pair of coupled wave equations^[3]:

$$\begin{aligned} (\nabla_t^2 - \beta^2 + k^2 n^2) e_x &= -\frac{\partial}{\partial x} \left(e_x \frac{\partial \ln n^2}{\partial x} + e_y \frac{\partial \ln n^2}{\partial y} \right) \\ (\nabla_t^2 - \beta^2 + k^2 n^2) e_y &= -\frac{\partial}{\partial y} \left(e_x \frac{\partial \ln n^2}{\partial x} + e_y \frac{\partial \ln n^2}{\partial y} \right) \end{aligned} \quad (1)$$

where $k = 2\pi/\lambda$ is the wave number, $n = n(x, y)$ the transverse refractive index profile, and β the propagation constant of the corresponding mode.

To solve the wave equations above, we employ a superlattice to describe the transverse refractive index profile^[3]. Because the modal fields of the guiding mode in PCF have the characteristics of localization, the localized Hermite-Gaussian functions are used as basis functions to decompose the electric field. Thus the vector wave e-

* This work was supported by the National High Technology Research Program of China (No. 2004AA31g200).

** E-mail: lousq@163.com

equations are deduced into the following eigenvalue systems:

$$\begin{bmatrix} L_1 & L_2 \\ L_3 & L_4 \end{bmatrix} = \beta^2 \begin{bmatrix} e_x \\ e_y \end{bmatrix} \quad (2)$$

where $L_1 = I_{abcd}^{(1)} + k^2 I_{abcd}^{(2)} + I_{abcd}^{(3)x}$, $L_2 = I_{abcd}^{(4)x}$, $L_3 = I_{abcd}^{(4)y}$, $L_4 = I_{abcd}^{(1)} + k^2 I_{abcd}^{(2)} + I_{abcd}^{(3)x}$; and $I^{(1)}$, $I^{(2)}$, $I^{(3)}$ and $I^{(4)}$ are overlap integrals of the modal functions defined in our previous work^[5]. It is a significant advantage in this way that all these integrals can be done analytically, and the numerical precision and efficiency can be improved greatly, especially when a great numbers of terms are needed in the expansions.

By solving Eq. (2) at a particular wavelength λ , the modes and the corresponding β of the PCF at a given wavelength λ can be calculated. The transverse modal electric field can be obtained by substituting the eigenvector into the decomposed equation.

In conventional fiber, modal effective index β/k_0 of guided mode is greater than n_{clad} , the index in the cladding and less than n_{core} in the core region. The same theory should also be applied to the PCF. The effective cladding index of PCF can be obtained by investigating the propagation of the fundamental cladding mode, which is also called the fundamental space filling mode (FSM) defined as the mode with the highest effective index in the cladding of infinite perfect PC^[6]. One of the efficient numerical models for analyzing FSM is plane wave expansion method (PWM)^[7].

Taking the PCF to be uniform in the propagation (z) direction, the modal magnetic field of infinite PC can be described by Helmholtz equation

$$\nabla \times \left[\frac{1}{\epsilon(r)} \nabla \times \right] H(r) = \left(\frac{\omega}{c} \right)^2 H(r) \quad (3)$$

where $\epsilon(r)$ is the dielectric constant, ω the angular frequency, and c the light velocity in vacuum.

According to the Bolch theory, the magnetic field can be expanded by plane wave as below:

$$\vec{H}(r) = \sum_{\vec{G}, u} h_{G,u} \hat{e}_u e^{i(\vec{k} + \vec{G} \cdot \vec{r})} \quad (4)$$

where u has two value of 1 and 2, \vec{G} is a vector in the reciprocal space, and \hat{e}_u represents two primitive vectors vertical to the propagation direction $\vec{k} + \vec{G}$. Three vector \hat{e}_1 , \hat{e}_2 , and $\vec{k} + \vec{G}$ are vertical to each other. $H_{G,u}$ is a component of the magnetic field in the direction \hat{e}_u . Dielectric constant can be expanded by Fourier series^[7]:

$$\begin{aligned} \epsilon(\vec{r}) &= \sum_{\vec{G}} \epsilon_G e^{i\vec{G} \cdot \vec{r}}, \\ \epsilon_G &= \frac{1}{V} \int_V \epsilon(\vec{r}) e^{-i\vec{G} \cdot \vec{r}} dV \end{aligned} \quad (5)$$

where V is the volume of primitive cell. Substituting equation (4) and (5) into (3), equation (3) becomes the algebraic eigenvalue problem:

$$\sum_{\vec{G}} | \vec{k} + \vec{G} | | \vec{k} + \vec{G} | \epsilon^{-1}(\vec{G}') - \vec{G}' \cdot \vec{G}' \begin{bmatrix} h_{1,G'} \\ h_{2,G'} \end{bmatrix} = \frac{\omega^2}{c^2} \begin{bmatrix} h_{1,G} \\ h_{2,G} \end{bmatrix} \quad (6)$$

Combining the method of full-vector based on the super-lattice and that of plane-wave expansion, we analyze the properties of the high birefringence PCF as shown in figure 1. The polarization degeneracy is lifted in two-fold rotational symmetry fibers, so that the fiber appears high birefringence. n_{eff}^x and n_{eff}^y are effective indices of the two orthogonal polarization states in the fundamental mode, respectively, corresponding to the slow and fast axis. The effective index n_{cl} in the cladding region is defined by the index of FSM that can be calculated by plane-wave expansion method. When n_{eff}^x or n_{eff}^y is larger than n_{cl} , the mode is a guiding mode. When n_{eff}^x or n_{eff}^y is smaller than n_{cl} , the mode becomes a leaky mode, where it is the cutoff of the fundamental mode. When n_{eff}^x is larger than n_{cl} and n_{eff}^y is smaller than n_{cl} , the fiber guides only one polarization mode- x polarization fundamental mode. Figure 2 shows the effective index curves of the x -polarized fundamental mode, y -polarized fundamental mode, and FSM as a function of wavelength for the PCF shown in figure 1, where $\Lambda = 2.55 \mu\text{m}$, $d_1/\Lambda = 0.3$ and $d_2/\Lambda = 0.833$. The x -polarized fundamental mode has higher effective index than that the y -polarized fundamental mode has. Therefore, the cut-off wavelength of x -polarized mode is longer than that of y -polarized mode. The y -polarized mode is unguided in the wavelength range over $1.4 \mu\text{m}$, and the x -polarized mode is unguided in the wavelength range over $1.6 \mu\text{m}$, there fore a single-mode single-polarization region within the

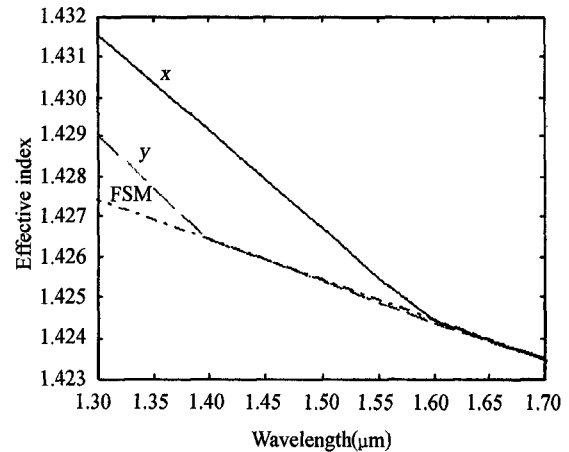


Fig. 2 Modal effective index of x -polarized mode, y -polarized mode and FSM for high Birefringence PCF with $\Lambda = 2.55 \mu\text{m}$, $d_1/\Lambda = 0.3$ and $d_2/\Lambda = 0.833$

wavelength from 1.4 μm to 1.6 μm is obtained, guided only by a x -polarized mode.

Figure 3 shows the intensity profile of the x -polarized fundamental mode at a wavelength of 1.55 μm , where intensity contours are spaced by 2 dB. The mode profile is well confined to the core region and elongated in the direction of direction x (slow axis). Mode field appears a shape of near ellipse and strongly linear polarization.

Modal birefringence is an important parameter for a high birefringence PCF. Figure 4 shows the modal birefringence of fundamental mode as a function of the wa-

velength in this PCF. There are two characteristic points, A and B, in figure 4. Point A represents the cut-off point of y -polarized mode and B is correspondent to the cutoff point of x -polarized mode. λ_A equals to 1.4 μm , λ_B equals to 1.6 μm , and the wavelength difference $\lambda_B - \lambda_A$ is 200 nm. The $\lambda_B - \lambda_A$ represents the bandwidth of the single-mode single-polarization wavelength region. When wavelength λ is less than λ_A , modal birefringence in the fiber increases monotonously with the increase of the wavelength, due to the field penetration further into the periodic cladding region. Modal birefringence of 1.8×10^{-3} is obtained at the wavelength 1.31 μm .

According to the numerical results, the mode cut-off could be judged by the relation between the effective index of two polarized fundamental mode and FSM. While the abrupt change in dispersion or birefringence curve can also be used for analyzing the mode cut-off.

A new type of high birefringence PCF is proposed in this paper. Due to the two different sizes of the holes introduced into the cladding of the PCF, the fiber is two-fold rotational symmetry and appears to be of high birefringence, which is much higher than that in the conventional polarization-maintaining fiber. When the ratio of the diameters of the big holes and the small holes is greater than 1, a W-type profile of effective index is constructed, and the cut-off of the fundamental mode will occur at the longer wavelength for the W-type fiber. According to the numerical result, we can obtain near 200nm SPSM region for the SPSM PCF with $\Lambda = 2.55 \mu\text{m}$, $d_1/\Lambda = 0.3$ and $d_2/\Lambda = 0.833$ and also get a modal birefringence of 1.8×10^{-3} at the wavelength 1.31 μm . There will be some new possibilities of fabricating high performance SPSM PCFs with this new type of high birefringence PCF.

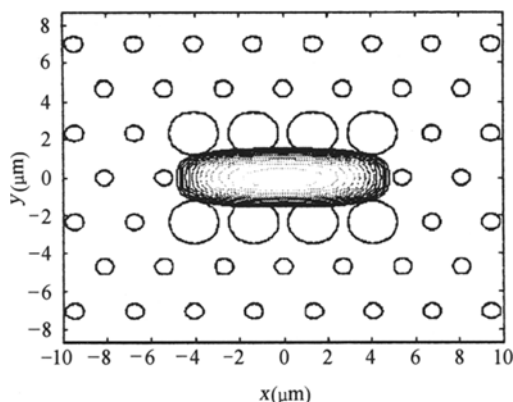


Fig. 3 Contour map of x -polarized modal field intensity at wavelength 1.55 μm for the high Birefringence PCF with $\Lambda = 2.55 \mu\text{m}$, $d_1/\Lambda = 0.3$ and $d_2/\Lambda = 0.833$

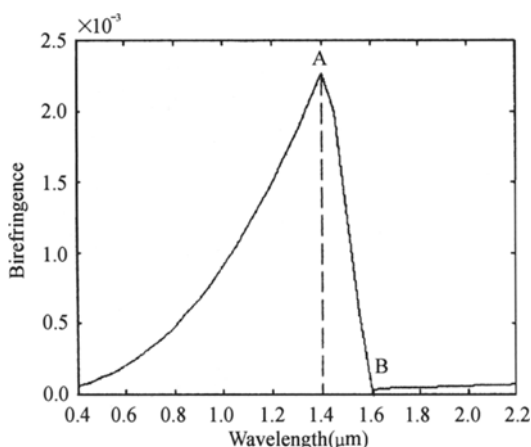


Fig. 4 Birefringence as a function of wavelength of the high Birefringence PCF with $\Lambda = 2.55 \mu\text{m}$, $d_1/\Lambda = 0.3$ and $d_2/\Lambda = 0.833$

References

[1] A. Ortigosa Blanch, J. C. Knight and W. J. Wadsworth. *Opt. Lett.*, **25**(2000), 1325.
 [2] Kunimasa Saitoh and Masanori Koshiba. *IEEE Photonic Tech. Lett.*, **14**(2002), 1291.
 [3] Lou Shuqin, Wang Zhi, Ren Guobin, and Jian Shuisheng. *Journal of Optoelectronics • laser*, **15**(2004), 1021. (in Chinese)
 [4] S. Kawakami and S. Nishida, *IEEE J. Quantum Electron*, **QE-10**, (1974), 879.
 [5] W. Zhi, R. G. Bin, L. S. Qin, and S. S. Jian. *Opt. Express*, **11** (2003), 980.
 [6] T. A. Birks, J. C. Knight, and P. St. J. Russell, *Opt. Lett.*, **22** (1997), 961.
 [7] S. Guo and S. Albin, *Opt. Express*, **11**(2003), 167.